RSC Advances

ROYAL SOCIETY OF CHEMISTRY

www.rsc.org/advances

RSC Advances

ARTICLE

Efficient oxygen electroreduction over ordered mesoporous Co-N-doped carbon derived from cobalt porphyrin

Received 00th January 20xx,
Accepted 00th January 20xx

DOI: 10.1039/x0xx00000x

www.rsc.org/

C. Li, Z. Han, Y. Yu, Y. Zhang, B. Dong, A. Kong*, and Y. Shan*

The demand for directly converting chemical energy generated by exothermal redox reactions into electrical energy has increased markedly in recent years and motivates the development of novel electrochemical power sources. The use of fuel cell technology may be the most promising solution for electrochemical propulsion in electric vehicles. However, at present, the design and synthesis of high-performance and low-cost catalysts for oxygen reduction reaction (ORR) still remain a significant challenge. Here, a high-performance Co-based carbon electrocatalyst (Co-N-GC) for ORR is prepared by a simple wet-impregnation nanocasting method using SBA-15 as hard templates and water-soluble cobalt porphyrin as precursors. The prepared catalysts with Co-N_x moieties have ordered mesoporous channels, and high special surface area and the degree of graphitization. In 0.1 M $HClO_4$ medium, the ORR over Co-N-GC prepared at the optimized heat-treatment temperature (800 °C) exhibits positive half-wave potential (0.79 V) and higher ORR current density (5.6 mA cm^{-2} at 0.2 V) comparable to commercial Pt/C (20 wt %) catalysts. Moreover, the prepared Co-N-GC materials possess the intrinsic long-time stability and the excellent methanol resistance toward ORR in both acidic and alkaline media, and may serve as a promising alternative to Pt/C materials for the ORR in the widespread implementation of fuel cell.

1. Introduction

Using nonprecious metal catalysts (NPMCs) for oxygen reduction reaction on the cathod of polymer electrolyte fuel cells (PEFCs) is more economical, and has important significance to the widespread implementation of PEFCs in the clean energy applications.[1] Extensive efforts have been made to explore the construction of NPMCs with the desired performance. A large amount of efficient NPMCs with the special morphology and architecture have been investigated in the past decades.[2-5] Among numerous NPMCs reported,[6-16] carbon-supported iron-nitrogen (Fe-N/C) and cobalt-nitrogen catalysts (Co-N/C) are believed to be the most promising alternatives to the platinum-based catalysts, due to their excellent electrocatalytic performance towards oxygen reduction reaction (ORR).[17-20] However, from a practical point of view in harnessing the chemical energy via direct electrochemical conversion, their electrocatalytic activity and stability are still insufficient and need to be further improved.

Some experimental investigation results illustrated that iron-based catalysts showed higher ORR activity than Co-based catalysts, but the latter usually exhibited higher catalytic stability.[21] Improving the catalytic activity of Co-N/C materials or increasing catalytic stability of Fe-N/C materials should be an effective way to develop highly efficient NPMCs that can gain satisfied result in practical use. Along this direction, the Fe-N/C electrocatalysts with high ORR performance were widely prepared by optimizing the synthesis parameters including species of precursors, heat-treatment temperatures, and carbon supports etc. However, there is only a limited progress on the activity enhancement of Co-based electrocatalysts. By choosing different nitrogen-containing organic compounds, for example, porphyrins, phthalocyanines, dibenzotetraazaannulenes, phenanthrolines, polypyrrole, triethylenetetramine chelate and tripyridyl triazine and optimizing the synthesis conditions such as the mole ratio of N to Co atoms, heat-treatment procedures and carbon supports, some synthesis routes were also explored for the preparation of high-performance Co-based NPMCs.[22-29] Among them, ORR half-potential of the best Co-based catalyst is about 10 mV lower than that of commercial Pt/C catalyst in alkaline medium and about 40 mV in acidic medium. It is still a challenge to prepare Co-based NPMCs with high ORR performance comparable to commercial Pt/C catalysts over a wide pH range of aqueous media.

Cobalt porphyrins with Co-N_4 moieties were widely used as the effective precursors for the preparation of Co and N co-doped carbon.[30-36] However, most of Co-N-C materials are prepared by the pyrolysis of carbon-supported cobalt porphyrin. The limited loading content for maintaining their well-dispersion on carbon supports and the stripping and aggregation phenomenon of active Co-nitrogen-carbon species and carbon supports often undermined the catalytic activity and stability of such Co-N-C materials. Recently, carbon-supported Co-N-C

School of Chemistry and Molecular Engineering, East China Normal University, 500 Dongchuan Road, Shanghai 200241, P.R. China. E-mail: ykshan@chem.ecnu.edu.cn (Y.Shan) and agkong@chem.ecnu.edu.cn (A.Kong)
Electronic Supplementary Information (ESI) available: [Fig S1, S2, S3 and S4; Table S1 and S2]. See DOI: 10.1039/x0xx00000x

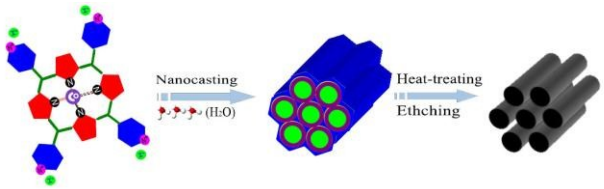

Fig. 1. The abridged general view of synthesis of Co-N-GC.

materials were prepared by thermally conversion of Co-porphyrin and believed to be highly efficient electrocatalyst for ORR, but which are well below the performance of the commercial Pt/C catalyst.[34-36]

Herein, a self-supported Co-N-doped mesoporous graphite catalyst (Co-N-GC) with comparable activity to commercial Pt/C catalyst in a wide pH range of aqueous media was obtained by a wet-impregnation nanocasting method previously reported by us (Fig. 1).[18-20] Water-soluble 5, 10, 15, 20-Tetra (4-pyridyl) cobalt porphyrin iodide (Co-porphyrin) is especially chosen as the only precursors to prepare this high-performance Co-based electrocatalysts. The prepared Co-N-GC has high accessible surface area and large-sized mesochannels for the convenient transportation of O_2. More importantly, the special Co-porphyrin precursors and the optimized heat-treatment temperatures created high density Co-N_x active sites in the graphite framework. As a result, the prepared catalysts show efficent electrocatalytic performance and high stability for the ORR in both alkaline and acidic media.

2. Experimental

2.1 Synthesis of Co-porphyrin

For the synthesis of the 5,10,15,20-tetra(4-pyridyl) cobalt porphyrin iodides (CoTPyPI), 2.0 g of 5,10,15,20-tetra(4-pyridyl) porphyrin (TPyP) and 4.0 g of $Co(AC)_2 \cdot 6H_2O$ were added in 100 mL of N,N-dimethyl-formamide (DMF), and then this mixture was refluxed for 24 h at 120 °C. The resulting CoTPyP products were collected by filtering and washed by ethanol. For the methylation of CoTPyP, the resultant CoTPyP (1.2 g) and methyl iodide (9.1 g) were mixed in 100 mL DMF and stirred for 12 h at 120 °C under reflux condition. After cooled to room temperature, 400 mL of acetone was added into the reaction mixtures. CoTPyPI products were separated by filtering, washed five times with acetone and then dried in vacuum oven at 60 °C.

2.2. Preparation of Co-N-GC

The Co-N-GC was prepared by a typical wet-impregnation nanocasting procedure. SBA-15 powders (0.5 g) was added into an aqueous solution consisting of acetic acid (10 mL), deionized water (20 mL), and Co-porphyrin (1.0 g). This mixture was stirred at 45 °C to evaporate the solvent in a fume cupboard. After the solvent was removed, the obtained brown powders were heated to 800 °C at a heating rate of 2 °C min^{-1} and held at 800 °C for 4 h in the tube furnace under N_2, Thereafter, the obtained samples were immersed in 5 wt % HF solution and stirred for 12 h at room temperature to remove the silica templates. The as-prepared Co-N_x-doped mesoporous material was designated as Co-N-GC-800. For comparison, Co-N-GC-700 and Co-N-GC-900 were also obtained at the corresponding heat-treatment temperatures by similar preparation procedures.

2.3. Electrode preparation and electrochemical measurement

The electrocatalytic activities of the as-prepared catalysts for ORR were evaluated by cyclic voltammetry (CV) and rotating disk electrode (RDE) techniques on the CHI-760C electrochemical analyzer. A three-electrode cell was employed incorporating a working glass carbon RDE (5 mm, Pine), an Ag/AgCl, KCl (3 M, 0.949 V vs. reversible hydrogen electrode in 0.1 M KOH solution and 0.268 V in 0.1 M $HClO_4$ solution) electrode as reference electrode, and a Pt electrode as counter electrode. For preparation of the working electrode, 10 mg Co-N-GC catalysts were dispersed in solvent mixtures containing 1.2 ml ethanol and 0.08 ml Nafion (5 %) under sonication to form a suspension. A little of such ink is pipetted onto the polished glassy carbon electrode surface and then dried at room temperature before measurement. For comparison, a commercially available Pt/C catalyst (20 wt %, Alfa) was also prepared using the same procedure. The experiments were carried out in O_2-saturated 0.1 M KOH solution and 0.1 M $HClO_4$ solution respectively.

The ORR current is obtained by subtracting the current measured in Ar-saturated electrolyte from the current measured in O_2-saturated electrolyte. The onset ORR potential was defined as the electrode potential when ORR current density is 3 μA cm^{-2} in RDE polarization curves, according to the reported method in the literature.[37,38] The Koutecky− Levich (K − L) equations have been used to calculate the kinetic parameters (Equation 1):

$$\frac{1}{J} = \frac{1}{J_L} + \frac{1}{J_K} = \frac{1}{B\omega^{1/2}} + \frac{1}{J_K};$$
$$B = 0.62nFC_0(D_0)^{2/3}\upsilon^{-1/6};$$
$$J_K = nFkC_0$$

In which J, J_K and J_L are the measured current density, kinetic- and diffusion-limiting current densities, respectively; ω is the angular velocity of the disk, n is the number of the electrons transferred in ORR, F is the Faraday constant (F= *96 485 C mol* L^{-1}), C_0 is the bulk solubility of O_2, D_0 is diffusion coefficient of O_2, v is the kinematic viscosity of the electrolyte, and k is the electron transfer rate constant. The number of electrons transferred (n) and J_K can be obtained from the slope and intercept of the K-L plots. The calibration of Ag/AgCl electrode with respect to reversible hydrogen electrode (*RHE*) can be seen in Fig. S1 in the supporting information.

2.4. Characterizations

Powder X-ray diffraction patterns (XRD) were recorded on a D8 advance diffractometer at the voltage of 40 kV.

Transmission electron microscopy (TEM) images were a JEM-

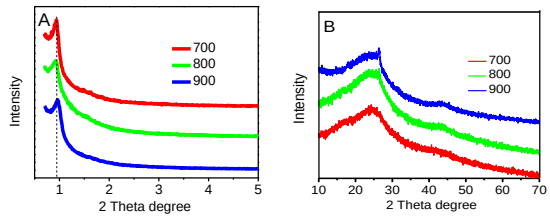

Fig. 2. The small-angle (A) and large-angle (B) XRD of mesoporous Co-N-GC-700, Co-N-GC-800, and Co-N-GC-900.

2010 transmission electron microscope at an acceleration voltage of 200 kV. N_2 adsorption/desorption isotherm measurements were carried out at 77 K on a Micromeritics ASAP 2020 analyzer. Specific surface areas were calculated by the Brunauer-Emmett-Teller (BET) method, and the pore size distributions were obtained from the related adsorption isotherms by using the Barrett-Joyner-Halenda (BJH) model. The X-ray photoelectron spectroscopy (XPS) measurements were performed on the instrument of Thermo ESCALAB 250 using Al Kα radiation (1486.6 eV). C 1s (284.6 eV) was utilized as a reference standard to correct the binding energy. A ST-4800 (Hitachi) scanning electron microscope (SEM) was used to investigate the morphology of the Co-N-GC catalysts. The metal contents for each catalyst were analyzed by inductively coupled plasma-atomic emission spectrometry (ICP-AES, IRIS Intrepid II).

3. Results and discussion

5,10,15,20-tetra(4-pyridyl) cobalt porphyrin iodide contains abundant pyridine-like nitrogen and carbon atoms as well as Co-N_4 moieties, which are beneficial for creating the highly active pyridine-like nitrogen atoms and Co-N_x moieties in the carbon matrixes for ORR in the mesoporous Co-N-GC material.[18-20,39] In addition, the better solubility of Co-porphyrin iodide in acetic acid aqueous solution facilitates the impregnation of this macrocycle molecule in the mesochannels of hard templates and supplies sufficient raw materials for replicating the inverted structure of SBA-15. Moreover, the confinement effect of channel in SBA-15 templates provides feasible control means to prepare Co-N-GC with high density of active sites and strong capability for mass- and charge-transport. As a result, highly efficient Co-N-GC materials for ORR were successfully prepared by such a special wet-impregnation nanocasting method.

The ordered mesoporous structures of Co-N-GC were confirmed by XRD, TEM and N_2-sorption analyses. A remarkable diffraction peak at about 2θ=0.9° was observed in the low-angle XRD patterns of Co-N-GC materials prepared at different temperatures, which attributed to the (100) reflections of hexagonal mesoporous structures (Fig. 2A). It suggested that ordered mesoporous Co-N-GC materials may be successful replicated from SBA-15 templates in a wide range of temperatures by a wet-impregnation method.[40] The corresponding SEM images (Fig. 3A) also exhibited the porous rod-shaped morphology, similar to that of the SBA-15 templates.[41] TEM images in Fig. 3B-D showed large domains with well-ordered hexagonal arrays of mesopore channels and further confirmed that the prepared Co-N-GC catalysts possess the ordered mesoporous structure.

For examining the degree of graphitization of pore wall in the Co-N-GC, the large-angle XRD patterns of Co-N-GC prepared at different temperatures were measured. The results were shown in Fig. 2B. Two broad peaks ascribing to the (002) and (101) diffraction of graphitic structure at 2θ=25 and 43° can be observed in Fig. 2B, which indicate the formation of graphitization in pore walls. The peak intensity at 2θ=25 and 43° increases with the increasing heat-treatment temperatures. It suggests that the higher heat-treatment temperatures can enhance the graphitization degrees of the Co-N-GC frameworks. At the same time, the SAED pattern (Fig. 3F) for Co-N-GC-800 shows clear diffraction rings of graphitic carbon in agree with

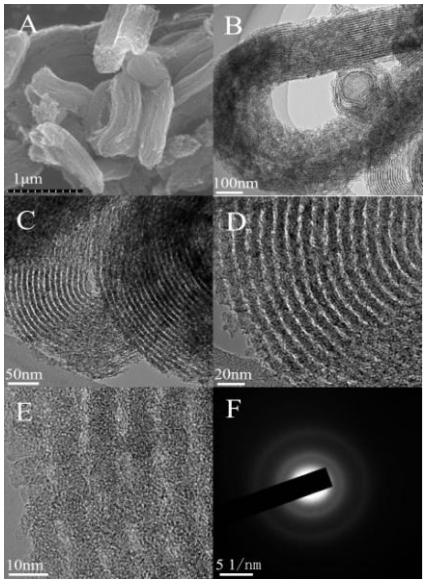

Fig. 3. SEM (A), TEM (B, C and D) and high-resolution TEM images (E) of the prepared Co-N-GC-800 and the corresponding selected-area electron diffraction images (SAED) (F).

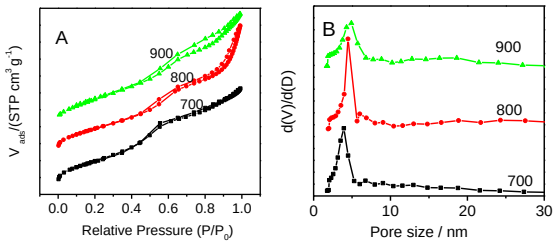

Fig. 4. (A) N_2-sorption isotherm curves and (B) the corresponding pore size distribution curves for the prepared Co-N-GC-700, Co-N-GC-800, and Co-N-GC-900.

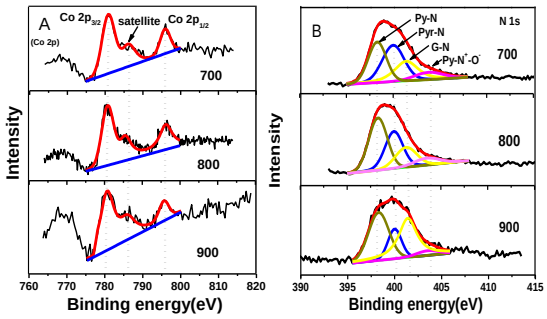

Fig. 5. (A) The XPS spectra of Co 2p; (B) N1s spectra for mesoporous Co-NG-C-700, Co-N-GC-800, and Co-N-GC-900.

the graphitic stripes in the high-resolution TEM image (Fig. 3E). These facts proved the appropriate graphitization of pore wall, which could contribute to the improvement of its electron conductivity.

N_2-adsorption and desorption isotherms illustrated that the prepared Co-N-GC materials at different temperatures exhibited type-IV isotherms of typical mesoporous material (Fig. 4A). The corresponding parameters are summarized in Table S1. Among the prepared Co-N-GC materials, Co-N-GC-700 has the highest BET surface area (723 m^2 g^{-1}). With the increasing heat-treatment temperature from 700 to 900 °C (Fig. 4B and Table S1), the pore sizes of the mesoporous Co-N-GC have a slight increasing from 3.9 to 4.7 nm, which also should be ascribed to the shrinkage of the pore walls at higher temperatures. Another prominent trait of the prepared Co-N-GC is the narrow pore-size distribution (Fig. 4B and TableS1). Such large-pore structures with high surface area may provide a desired support for the catalytic active sites and facilitate the transportation of O_2 and infiltration of electrolyte.

The distribution, the content and chemical environment of the component elements in the surface of the prepared mesoporous Co-N-GC material strongly influence its catalysis activity and the structural stability of active sites. The investigated SEM-EDS mapping revealed a uniform distribution of Co, N, C and O atoms in the surface of these Co-N-GC materials (Fig. S2). Its uniform distribution is obviously different from the analogue materials reported in the literature, such as metal complex decorated ZIF materials,[42] N-self-doped graphene-based nonprecious Fe catalyst (Fe-N-graphene),[43] catalysts prepared by pyrolyzing various metal-nitrogen-carbon precursors,[44] CoDETA/C catalyst prepared by pyrolyzing cobalt diethylenetriamine chelate on carbon.[45] The soluble Co-porphyrin complexes as the precursors may easily be filled into the channels of hard templates, efficiently decrease the formation of non-uniform mesostructured structures and large bulk particles and give an opportunity to enhance their density of active sites.

Typically, the XPS results (Table S2) reveal that the Co-N-GC-800 is composed of C, N, O, and Co. The surface N (6.8 at %) and Co (0.6 at %) content of Co-N-GC-800 (Table S2) is relatively higher than those of the previously reported materials containing Co and N.[11,46] The Co content in Co-N-GC catalysts have also been measured by ICP-AES measurements. The weight percentage of Co in Co-N-GC-700, Co-N-GC-800 and Co-N-GC-900 is 3.4, 3.6 and 1.8 wt %, respectively (See ESI). The lower content of Co in Co-N-GC-900 mainly is due to the degradation of Co-N_x species and formation of Co metal particles at higher temperature, which were leached by HF solution in the preparation process. Three peaks at 780.6 (Co $2p_{3/2}$), 785.4(satellite peak) and 796.2 (Co $2p_{1/2}$) eV in the XPS spectrum of Co 2p in Fig.5 were clearly observed and are similar to the Co 2p XPS of other catalysts containing Co^{2+} in the literature.[47-49] The deconvolution of the N 1s signals gives four peaks with binding energies centred at 398.3, 400.0, 401.2 and 403.5 eV (Fig. 5B), which may be assigned to pyridinic-N (Py-N), pyrrolic-N (Pyr-N), graphitic-N (G-N), and N-O (Py-N^+-O^-) species, respectively.[50,51] Pyridinic and pyrrolic nitrogen atoms can associate with Co ions in the mesoprous framework to form active Co-N_x species for ORR.[20,21] The Uv-vis diffuse reflection spectrum of Co-N-GC-800 reveals four weak absorption peaks at 458, 560, 586 and 604 nm (Fig. S3). These peaks are the similar to those of Co porphyrin precursor and the results in the literature[52], and may be assigned to the Co-N_x moiety. It could further confirm the formation of Co-N_x active site in the Co-N-GC-800.

Moreover, the relative content of Co and different types of doped nitrogen in the surface of Co-N-GC is also displayed in Table S2. It also can be seen that the N-graphitic groups possess the higher thermodynamic stability than pyridinic and pyrrolic N groups, just like the description in the literature.[53,54] However, the relative amount of pyridinic-N increases with the heat-treatment temperature rising and reach to the maximum value around 800 °C, and then decrease in the

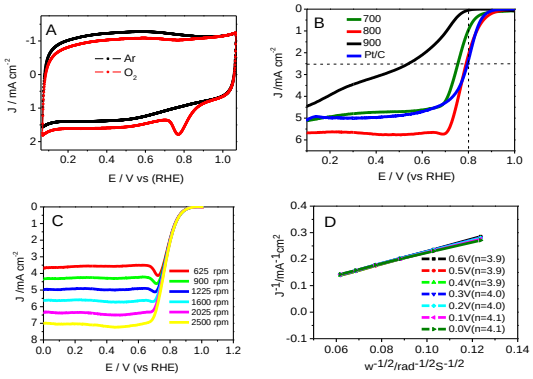

Fig. 6. (A) CVs of Co-N-GC-800 in a Ar-saturated, or O_2-saturated 0.1 M $HClO_4$ solution; (B) RDE polarization curves of Co-N-GC materials and Pt/C at 1600 rpm in an O_2-saturated 0.1 M $HClO_4$ solution; (C) RDE polarization curves of Co-N-GC-800 at different rotation rates in an O_2-saturated 0.1 M $HClO_4$ solution; (D) Koutecky-Levich plot (J_L^{-1} versus ω^{-1}) of Co-N-GC-800 at different potentials. The loadings of catalyst on the electrode are 0.6 mg cm^{-2} for Co-N-GC materials and 0.1 mg cm^{-2} for Pt/C electrode. For all the measurements, the scan rate is 10 mV s^{-1}.

prepared samples. This variation tendency is the same as that of Co content in the samples with the heat-treatment temperature rising. It seems to testify that the presence of Co may stabilize pyridinic-N groups in the surface of Co-N-GC. However, increasing the heat-treatment temperature to 900 ℃, the degradation and conversion of Co stabilized-pyridinic-N species obviously occurred because of the reduction of the Co ions and led to the decrease of pyridinic-N groups and Co in the surface (the generated Co metal was etched off by acid). The higher content of pyridinic-N and Co in Co-N-GC-800 may contribute to its higher activity for ORR.[46]

CV experiments over Co-N-GC-800 (Fig. 6A) revealed an obvious diffusion-controlled ORR peak at 0.78 V (*vs. RHE*) in O_2-saturated 0.1 M $HClO_4$ solution[55] and is absent in the electrolyte saturated with Ar. Linear sweep voltammetry measurements (LSV) are carried out to evaluate the catalytic performance of the Co-N-GC samples prepared at different temperatures for ORR in 0.1 M $HClO_4$ electrolyte. It can be seen (Fig. 6B) that the Co-N-GC-800 has the highest half-wave potentials ($E_{½}$) and shows the highest catalytic activity for ORR among three Co-N-GC samples. It is reported that Fe-based carbon electrocatalysts have high catalytic performance comparable to Pt/C catalyst in acidic medium, but it is scare for Co-based ORR catalysts. The ORR half-wave potential ($E_{½}$) on the preapred Co-N-GC by us reaches 0.79 V with the catalyst loading of 0.6 mg cm^{-2}, very close to that of Pt/C (20 wt %, Alfa) catalyst (0.81 V, same with that on Pt/C catalysts in literature[48]) (Fig. 6B). Moreover, the measured current density over the Co-N-GC-800 electrode at 0.2 V is 5.6 mA cm^{-2}, slightly higher than that over the commercial Pt/C (20 wt %, Alfa) (4.9 mA cm^{-2} ; catalyst loading: 0.1 mg cm^{-2}) (Fig. 6B). These results indicated that the activity of the Co-N-GC-800 is comparable to the Pt/C catalysts and higher than some Co-based catalysts such as Co-Nx-C (E_p = 0.71 V),[20] CoDETA/C catalyst (E_p = 0.72 V),[45] PANI-Co-CNT (E_p = 0.62 V),[56] Co-PPy-TsOH/C (E_p = 0.69 V)[57] for ORR in acidic medium (E_p: *Peak potential*).

Moreover, the catalytic performance of the prepared Co-N-GC for ORR was also investigated in 0.1 M KOH electrolyte saturated with O_2. The results testify that Co-N-GC-800 has the highest activity for ORR among three Co-N-GC samples (Fig. S4) A well-defined cathodic peak appears at around 0.83 V (*vs. RHE*) in CV curve over Co-N-GC-800 in the electrolyte saturated with O_2 and is absent in the electrolyte saturated with Ar, as shown in Fig. 7A. The ORR half-wave potential on Co-N-GC-800 (0.81 V) is only slightly more negative than that over Pt/C (20 wt %, Alfa; Fig. 7B) catalyst (0.82 V, same with that on Pt/C catalysts reported in literature[52]). However, this $E_{½}$ value is significantly superior to previously reported Co-N/C materials, Co-N-GN ($E_{½}$ = 0.78 V),[58] Co-N-C900 ($E_{½}$ = 0.78 V).[59] The ORR current density on Co-N-GC-800 electrode measured at 0.8 V is 3.0 mA cm^{-2} with catalyst loading of 0.2 mg cm^{-2} and close to that on Pt/C (3.1 mA cm^{-2}; catalyst loading: 0.1 mg cm^{-2}) (Fig. 7B). These facts have sufficiently displayed the high intrinsic activity of Co-N-GC-800 for ORR in a wide pH range of aqueous values.

Higher catalytic activity of Co-N-GC for ORR mainly attribute to the optimized balance between the performance of activity sites, the amount of active site, and the transportation of electron and substrate. With the increasing of the heat-treatment temperature, the graphitization degree of carbon walls in the Co-N-GC is improved and is beneficial to the transportation of electron. However, the higher temperature also generally facilitates the degradation or removal of active Co and N species and leads to the content of them decreases. For example, when heat-treatment temperature increases from 700 to 800 ℃, the content of Co decreases from 0.5 to 0.2 at % and from 8.1 to 3.5 at % for N in the prepared Co-N-GC as shown in Table S2. At the same time, the surface area decrease from 723 to 622 m^2 g^{-1} (Table S2). Although Co-N-GC-900 has the higher degree of graphitization than Co-N-GC-800, both the lower active Co and N content (especially Co-N_x species) and the lower surface area contributed to the lowest activity among the prepared Co-N-GC materials. For Co-N-GC-700, the lower graphitization degree of carbon framework and the relative low amount of Co-N_x species were detrimental to its catalytic activity for ORR. As a result, Co-N-GC-800 showed the most optimized activity for ORR in both acidic and alkaline media. In addition, higher ORR activity of Co-N-GC-700 than Co-N-GC-900 should be ascribed to its higher active N and Co content (especially Co-N_x species) and the larger surface area.

Because Co-N-GC-800 material possesses excellent activity for ORR, the ORR kinetic process on it has also been investigated in both alkaline and acidic media. Firstly, polarization curves at different rotating speeds were recorded from 0 to 1.1 V with a scan rate of 10 mV s^{-1} to study the kinetics of the catalyzed ORR over Co-N-GC-800 in 0.1 M $HClO_4$ electrolyte (Fig. 6C). The current densities sharply increase with the rotating speeds (from 400 to 2500 rpm) in the

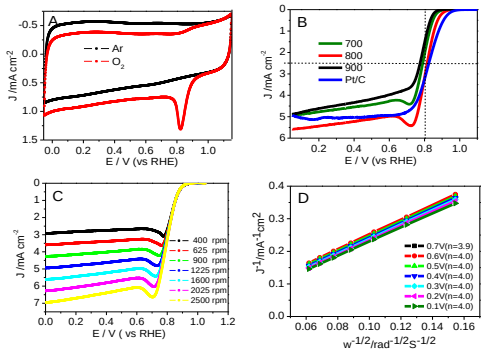

Fig. 7. (A) CVs of Co-N-GC-800 in a Ar-saturated or O_2-saturated 0.1 M KOH solution; (B) RDE polarization curves of Co-N-GC materials and Pt/C at 1600 rpm in an O_2-saturated 0.1 M KOH solution; (C) RDE polarization curves of Co-N-GC-800 at different rotation rates in an O_2-saturated 0.1 M KOH solution; (D) Koutecky – Levich plot (J_L^{-1} versus ω^{-1}) of Co-N-GC-800 at different potentials. The loadings of catalyst on the electrode are 0.2 mg cm^{-2} for Co-N-GC materials and 0.1 mg cm^{-2} for Pt/C electrode. For all the measurements, the scan rate is 10 mV s^{-1} .

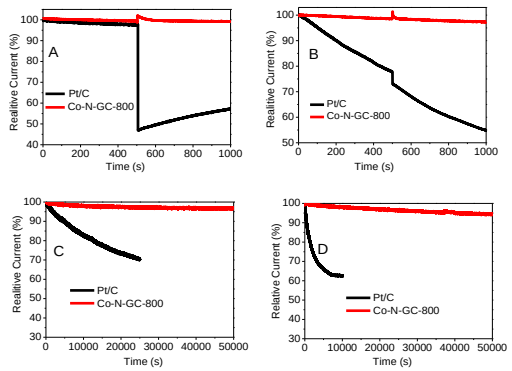

Fig. 8. Chronoamperometric responses of the prepared Co-N-GC-800 and Pt/C with addition of methanol A) in O_2 -saturated 0.1 M KOH; B) in O_2-saturated 0.1 M $HClO_4$. Chronoamperometric response of the prepared Co-N-GC-800 and Pt/C; C) in O_2 -saturated 0.1 M KOH; D) in O_2-saturated 0.1 M $HClO_4$. The loadings of Co-N-GC-800 on the electrode are 0.2 mg cm^{-2} in 0.1 M KOH and 0.6 mg cm^{-2} in 0.1 M $HClO_4$ electrolytes. The loadings of Pt/C electrode is 0.1 mg cm^{-2} in both electrolytes.

mixed kinetic-diffusion control region in the potential range of 0.7 to 0.9 V , indicating an efficient diffusion of the reactants in the catalysts, followed by a hump peak at the LSV of this Co-N-GC in both alkaline and acidic media. This phenomenon maybe arises from the insufficient compensation of O_2 concentration adsorbed on the inner surface of the catalyst layer after the accumulative oxygen within the catalyst layer by adsorption is depleted at more negative potential, which is similar to the results reported in the literature. [60,61] The subsequent current plateau exhibits a diffusion-limited kinetic process for ORR in the potential range of 0 to 0.6 V (Fig. 6B,C). To further explain the ORR catalyzed by Co-N-GC-800 modified electrodes, the LSV data were analyzed using the Koutecky-Levich (K-L) equation (Equation 1). The corresponding K-L plots from the RDE polarization curves over Co-N-GC-800 in 0.1 M $HClO_4$ electrolyte (Fig.6D) exhibited good linearity between 0 and 0.6 V. The number of electron transferred was calculated to be 3.9 on the basis of the K-L equations at 0.5 V (vs. RHE) $B=0.62nFC_0(D_0)^{2/3}v^{-1/6}$, $C_0= 1.18\times 10^{-3} mol\ L^{-1}$, $D_0= 1.9\times 10^{-5}\ cm\ s^{-1}$, $v= 0.0893\ cm^2s^{-1}$).[62] The same phenomena also have been observed in the in alkaline medium (Fig. 7C). The K-L plots in 0.1 M KOH electrolytes also exhibited good linearity from 0.1 to 0.7 V (Fig. 7D). The corresponding number of electron transferred at 0.6 V (*vs. RHE*) was calculated to be 4.0 using the K-L equation $B=0.62nFC_0(D_0)^{2/3}v^{-1/6}$, $C_0= 1.2\times 10^{-3}\ mol\ L^{-1}$, $D_0= 1.9\times 10^{-5} cm\ s^{-1}$, $v= 0.01\ cm^2s^{-1}$).[63] These facts verify that Co-N-GC-800 can efficiently catalyze the reaction of oxygen reduction by in a direct nearly four-electron-reduction pathway at low overpotential in acid and alkaline media.

The methanol-tolerance of the cathode catalyst is one of the major concerns in a direct-methanol fuel cell. To examine the effect of methanol crossover on the cathode behavior, we investigate the electrocatalytic selectivity of the prepared Co-N-GC catalysts and Pt/C against the oxidation of methanol in both O_2-saturated alkaline (0.1 M KOH) and acidic (0.1 M $HClO_4$) media in the presence of methanol (the final concentration of methanol injected into the electrolyte is 3.0 M). After the injection of methanol, no significant changes are observed in the ORR current density over Co-N-GC-800 catalysts in both acidic (Fig. 8B) and alkaline media (Fig. 8A). But whether in acidic or alkaline medium, the ORR current density over the commercial Pt/C catalyst significantly decreases (Fig. 8A and B), because of its inherent disadvantage of Pt electrocatalyst that has vulnerability to methanol attack.[64] The experimental results demonstrate that the Co-N-GC-800 catalysts possess the selectivity for ORR and methanol-tolerance performance superior to Pt/C catalyst.

The investigated results for the durability of the prepared Co-N-GC-800 catalyst in acidic and alkaline media were shown in Fig. 8 C and D. From the corresponding chronoamperometric, it can be seen that after running for 50, 000 s in 0.1 M KOH and 0.1 M $HClO_4$, it shows insignificant decay (about 2 % and 5 %) in current density on the Co-N-GC-800 electrodes at 0.55 and 0.57 V. The commercial Pt/C catalyst suffers from 30 % loss of current density after running for 25, 000 s in 0.1 M KOH (Fig. 8C) and 37 % loss after running for 10, 000 s in 0.1 M $HClO_4$ (Fig. 8D). Thus the durability of the prepared Co-N-GC-800 electrodes is not only higher than the commercial Pt/C catalyst, but also better than many analogous Co-based catalysts, Co/N-C-800 (retains a relative current of 95.8 % after 10 000 s in O_2-saturated 0.1 M KOH),[65] $Co_{1.12}/N_{2.92}$/C-700 (retains a relative current of 90.5 % and 86 % after 18 000 s in O_2-saturated 0.1 M KOH and 0.1 M $HClO_4$ respectively).[66]

4. Conclusions

In summary, we have successfully fabricated an efficent Co-based carbon electrocatalyst for ORR in a wide pH range. By a wet-impregnation nanocasting method with a water-soluble macromolcules containing Co-N_x moieties as the only precursor, the prepared Co-N-GC catalyst with ordered mesoporous exhibited high degree of graphitization, a high accessible surface area and large-pore channels for the transportation of electron O_2. The special precursor and the optimized heat-treatment process created high density ORR active sites in the graphite framework of the catalysts. The CV and RDE polarization curves confirmed positive ORR $E_{½}$ values and higher current density of the Co-N-GC-800 Co-based electrocatalysts in 0.1 M $HClO_4$ and 0.1 M KOH electrolyte, comparable to commercial Pt/C. This Co-N-GC-800 catalyst could somehow steer a complete reduction of O_2 to H_2O in four-electron process, and exhibit long-time stability toward ORR in both media as well as the excellent methanol resistance. This Co-based catalyst may serve as a promising alternative to Pt/C catalysts for the ORR in the widespread implementation of PEFCs.

Acknowledgements

The authors are grateful to financial support from China National Natural Science Foundation (No. 21303058), Shanghai Municipal Natural Science Foundation (No. 13ZR1412400), and the key project of Shanghai Science and Technology Committee (No. 11JC1403400 and 14231200300).

Notes and references

1 G. Wu and P. Zelenay, *Accounts chemi. Resa.*, 2013, **46**, 1878-1889.
2 F. Jaouen, E. Proietti, M. Lefevre, R. Chenitz and J.P. Dodelet, *Energy Environ. Sci.*, 2011, **4**, 114-130.
3 Z. Chen, D. Higgins and A. Yu, *Energy Environ. Sci.*, 2011, **4**, 3167-3192.
4 A. Rabis, P. Rodriguez and T.J. Schmidt, *ACS Catal.*, 2012, **2**, 864-890.
5 G. Wu, G.F. Cui and D.Y. Li, *J. Mater. Chem.*, 2009, **19**, 6581-6589.
6 C.H. Choi, C. Baldizzone and J.P. Grote, *Angew. Chem., Int. Ed.*, 2015, **54**, 12753-12757.
7 S. Wang, M. Zhu and X. Bao, *ChemCatChem*, 2015, **7**, 2937-2944.
8 Y. W. Ju, S. Yoo and C. Kim, *Adv. Sci.*, 2015.
9 J. Sa, C. Park, H.Y. Jeong, S.H. Park, Z. Lee, K.T. Kim, G.G. Park and S.H. Joo, *Angew. Chem., Int. Ed.*, 2014, **53**, 4102-4106.
10 D. Zhou, L. Yang and L. Yu, *Nanoscale*,2015, **7**, 1501-1509.
11 J.H. Lee, M.J. Park and S.J. Yoo, *Nanoscale*, 2015, **7**, 10334-10339.
12 Y. Zhai, C. Zhu and E. Wang, *Nanoscale*, 2014, **6**, 2964-2970.
13 Z. Liu, L. Ji and X. Dong, *RSC Adv.*, 2015, **5**, 6259-6264.
14 Z. Ma, C. Guo, Y. Yin, Y. Zhang, H. Wu and C. Chen, *Electrochim. Acta*, 2015, **160**, 357-362.
15 P.D. Tran, A. Morozan and S. Archambault. *Chem. Sci.*, 2015, **6**, 2050-2053.
16 L.Yang, N. Larouche and R. Chenitz, *Electrochim. Acta*, 2015, **159**, 184-197.
17 G. Wu, K.L. More, C.M. Johnston and P. Zelenay, *Science*, 2011, **332**, 443-447.
18 A.G. Kong, B. Dong, X.F. Zhu and Y.K. Shan, *Chem. Eur. J*, 2013, **19**, 16170-16175.
19 A.G. Kong, X.F. Zhu, Z. Han and Y.K. Shan, *ACS Catalysis*, 2014, **4**, 1793-1800.
20 A.G. Kong, Y.Y. Kong, X.F.Zhu and Y.K. Shan, *Carbon*, 2014, **78**, 49-59.
21 S. Li, L. Zhang and J. Kim, *Electrochim. Acta*, 2010, **55**, 7346-7353.
22 R. Jasinski, *Nature*, 1964, **201**, 1212-1213.
23 A. Widelov, *Electrochim. Acta*, 1993, **38**, 2493-2502.
24 G. Lalande , G. Faubert, R. Cote, D. Guay and J.P. Dodelet, *J. Power Sources*, 1996, **61**, 227-237.
25 F. Jaouen, M. Lefevre, J.P. Dodelet and M. Cai, *J. Phys Chem B*, 2006, **110**, 5553-5558.
26 C.W.B. Bezerra, L. Zhang, K. Lee, H. Liu, A.L.B. Marques, E.P. Marques, H. Wang and J. Zhang, *Electrochim. Acta*, 2008, **53**, 4937-4951.
27 G. Faubert, R. Côté, J.P. Dodelet, M. Lefèvre and P. Bertrand, *Electrochim. Acta*, 1999, **44**, 2589-2603.
28 H.J. Zhang, X. Yuan , W. Wen, D.Y. Zhang , L. Sun, Q.Z. Jiang and Z.F. Ma, *Electrochem Commun*, 2009, **11**, 206-208.
29 K. Asazawa, H. Kishi and H. Tanaka, *J. Phys. Chem. C*, 2014, **118**, 25480-25486.
30 C. Shi, B. Steiger, M. Yuasa, F.C. Anson, *Inorg. Chem*., 1997, **36**, 4294-4295
31 C.N. Shi, F.C. Anson, *Inorg. Chem.*, 1998, **37**, 1037-1043
32 F.C. Anson, E.H. Song, C.N. Shi, *Langmuir*, 1998, **14**, 4315-4321
33 M. Yuasa, R. Nishihara, C. Shi, F.C. Anson, *Polym. Adv. Technol.* 2001, **12**, 266-270
34 H. Tang, H. Yin, J. Wang, *Angewandte Chemie*, 2013, **125**, 5695-5699.
35 J.M. You, H.S. Han, H.K. Lee, *Int. J. Hydrogen Energy*, 2014, **39**, 4803-4811.
36 N.C. Cheng, C. Kemna, S. Goubert-Renaudin, A. Wieckowski, *Electrocatalysis*, 2012, **3**, 238-251
37 M. Chokai, M. Taniguchi, S. Moriya, K. Matsubayashi and T. Shinoda, *J. Power Sources*, 2010, **95**, 5947-5951.
38 Y. Hu, X. Zhao, Y. Huang, Q. Li and N.J. Bjerrum, *J. Power Sources*, 2013, **225**, 129-136.
39 W. Orellana, *J. Phys. Chem. C*, 2013, **117**, 9812-9818.
40 S. Jun, S.H. Joo, R. Ryoo, M. Kruk and M. Jaroniec, *J. Am. Chem. Soc.*, 2000, **112**, 10712-10713.
41 D. Zhao, J. Feng and Q. Huo, *science*, 1998, **279**, 548-552.
42 D. Zhao, J.L. Shui and L.R. Grabstanowicz, *Adv. Mater.*, 2014, **26**, 1093-1097.
43 C. He, J.J. Zhang, P.K. Shen, *J. Mater. Chem. A*, 2014, **2**, 3231-3236.
44 U. Tylus, Q. Jia and K. Strickland, *J. Phys. Chem. C*, 2014, **118**, 8999-9008.
45 H.J. Zhang, H. Li and X. Li, *Int. J. Hydrogen. Energ.*, 2014, **39**, 267-276.
46 L. Osmieri, A. H. A. M. Videla and S. Specchia, *J. Power Sources*, 2015, **278**, 296-307.
47 Z. Yin, T. Hu, J. Wang, *Electrochim. Acta*, 2014, **119**, 144-154.
48 X. Yuan, H.C. Kong, Y.J. He, *Int. J. Hydrogen Energy*, 2014, **39**, 16006-16014.
49 W. Bian, Z. Yang, P. Strasser, *J. Power Sources*, 2014, **250**, 196-203.
50 S. Jiang, C. Zhu and S. Dong, *J. Mater. Chem. A*, 2013, **1**, 3593-3599.
51 Y. Zhai, C. Zhu and E. Wang, *Nanoscale*, 2014, **6**, 2964-2970.
52 M. Shen, L.R. Zheng and W. He, *Nano Energy*, 2015, **17**, 120-130.
53 M. Favaro, L. Perini, S. Agnoli, *Electrochim. Acta*, 2013, **88**, 477-487.
54 V. Perazzolo, C. Durante, R. Pilot, *Carbon*, 2015, **95**, 949-963.
55 R.H. Wopschall, *Anal. Chem.*, 1967, **39**, 1514-1527.
56 Z. Yin, T. Hu and J. Wang, *Electrochim. Acta*, 2014, **119**, 144-154.
57 X. Yuan, H.C. Kong and Y.J. He, *Int. J. Hydrogen Energy*, 2014, **39**, 16006-16014.
58 S. Jiang, C. Zhu and S. Dong, *J. Mater. Chem. A*, 2013, **1**, 3593-3599.
59 Y. Zhai, C. Zhu and E. Wang, *Nanoscale*, 2014, **6**, 2964-2970.
60 W. Wei, H. Liang, K. Parvez, *Angew Chem.*, 2014, **126**, 1596-1600.
61 H.D. Sha, X. Yuan, X.X. Hu, J. Electrochem. Soc., 2013, **160**, F507-F513.
62 M. Shen, L.R. Zheng and W. He, *Nano Energy*, 2015, **17**, 120-130.
63 R. Liu, D.Wu and X. Feng, *Angew Chem.*, 2010, **122**, 2619-2623.
64 Z. H. Wen, J. Liu and J.H. Li, *Adv. Mater.*, 2008, **20**, 743-747.
65 Y. Su, Y. Zhu and H. Jiang, *Nanoscale*, 2014, **624**, 15080-15089.
66 Y. Yang, J. Liu and Y. Han, *Phys. Chem. Chem. Phys.*, 2014, **16**, 25350-25357.

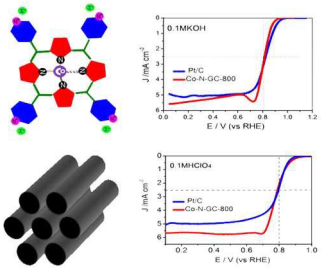

High-performance self-supported Co-N-doped carbon electrocatalyst for ORR with comparable activity to Pt/C in both acidic and alkaline media was prepared.